ISSN 2706-655X Vol.5, Issue 8: 71-80, DOI: 10.25236/IJFET.2023.050810

Study on Bubble Motion Characteristics in Transformer Oil under Non-Uniform Electric Field

Jingbo Zhang

International College and Engineering, Changsha University of Science & Technology, Changsha, 410000, China

Abstract: *The presence of bubbles and impurities, influenced by various external factors, has a significant impact on the operational condition of the transformer. In this study, a two-phase flow model with rod-plate electrodes was constructed based on the phase-field method to characterize the spatial distribution of non-uniform electric fields under the coupled effects of electric, thermal, and fluid fields. Numerical simulations were performed to analyze the effects of bubble size, number, and different voltage levels on bubble deformation, motion trajectory, and the extent of internal electric field distortion. The results indicate that during the vertical ascent phase, the bubbles undergo deformation perpendicular to the electric field direction, and during the slope ascent phase, they deform along the electric field direction. With an increase in voltage level, the stretching and repulsion of the bubbles by the electric field force also increase. There is a positive correlation between bubble size, voltage level, and the degree of distortion of the maximum electric field strength inside the bubbles. Coalescence of multiple bubbles leads to irregular shape changes and non-uniform distribution of polarized charge on their surface. However, the internal maximum electric field strength tends to increase with an increasing number of bubbles.*

Keywords: *Non-uniform electric field, bubbles, transformer oil, dynamical behavior*

1. Introduction

Transformers serve as essential equipment for power transmission and regulation in the power system, exerting a significant impact on its overall performance. Ensuring the stable operation of transformers holds great significance for the normal functioning of the power system. Oil-immersed transformers represent the predominant type of large-scale transformers utilized in domestic applications. Throughout their operation, transformer oil is subject to environmental factors, such as electric fields, temperature variations, and material aging, resulting in the emergence of impurities, particularly bubbles [1], [2], [3]. These impurities notably affect the operational condition of transformers. Suspended bubbles, a typical impurity found in transformer oil, exhibit significantly lower dielectric constant and conductivity than the oil itself. Consequently, this disparity leads to a higher electric field intensity within the bubbles. Nevertheless, bubbles have a lower withstand voltage than transformer oil, rendering them susceptible to partial discharge phenomena. This occurrence can result in oil degradation, compromised insulation performance, and potentially severe transformer failures. Therefore, conducting comprehensive research on the motion characteristics of bubbles in transformer oil proves valuable in assessing their effect on the oil's insulation performance.

Regarding the characteristics of bubble generation, J.P. Hill proposed a new model for predicting the Bubble Initiation Temperature (BIT) using data fitting methods [4]. Building upon the study of the initiation temperature of bubble escape (ITBE), Liu Yunpeng investigated the microstructure of paperboard and the mechanisms of bubble generation to establish a bubble evolution model for estimating ITBE [5]. Zhao Tao conducted numerical simulations to study the dynamic behavior of bubbles between plate electrodes in transformer oil under power frequency AC voltage. The results suggest that bubble aggregation may occur at the equilibrium position between the electrodes [6]. Liu Qiushi analyzed the motion characteristics of bubbles between cone-electrodes under extremely non-uniform AC voltage by considering the influence of bubble deformation and flow field, using experiments and numerical simulations. The results indicated that, under high electric field intensity, small bubbles tend to aggregate and form bubble clusters, eventually resulting in the formation of bubble bridges [7]. Yang Hao utilized numerical simulations and experimental simulations to analyze the trajectory and vertical velocity variation of bubbles under extremely non-uniform electric fields, focusing on bubble motion and

ISSN 2706-655X Vol.5, Issue 8: 71-80, DOI: 10.25236/IJFET.2023.050810

deformation [8]. Building upon the previous findings, Ladislas investigated the migration characteristics of bubbles in oil under the coupling effects of electric and the vibration fields, considering the influence of vibration field on bubble motion and deformation. The findings demonstrated that under the combined action of AC stress and vibration stress, bubbles undergo simultaneous stretching and oscillatory behavior, resulting in an intensified level of bubble distortion [9]. Previous studies have primarily focused on the generation, aggregation, deformation, and motion characteristics of bubbles in liquid phases within a homogeneous electric field. However, these studies did not account for the complex non-uniform electric field model present in the actual internal structure of transformers.

In summary, this paper constructed a rod-plate electrode gas-liquid two-phase flow model based on the phase-field method, which describes the spatial distribution of non-uniform electric fields under the coupling of electric, thermal, and fluid fields. Numerical simulations were employed to investigate the effects of bubble size, number, and different voltage levels on bubble deformation, motion trajectory, and the extent of internal electric field distortion.

2. Investigation of Bubble Motion Characteristics

2.1 Electric-Thermal-Fluid Coupling Principles

2.1.1 Coupled equations for the thermal and flow fields

During practical operation, transformers generate significant heat from core losses and resistive losses. The transformer oil absorbs most of the heat through heat convection, conduction, and radiation. As a result, the temperature of the bubbles in the oil fluctuates with the oil temperature. Furthermore, the flow of transformer oil transports and exposes the bubbles to the effect of the flow field. Fig. 1 illustrates the coupled model of the thermal and flow fields.

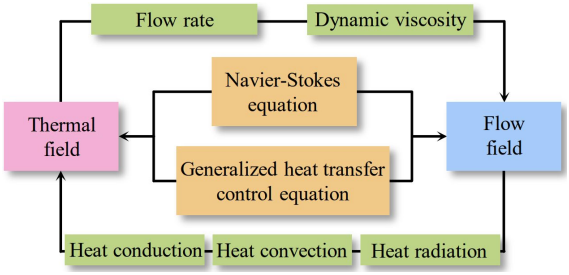

Figure 1: Coupled model of thermal and flow fields in transformer oil with bubbles

In this study, transformer oil is treated as an incompressible, immiscible, and non-Newtonian fluid, serving as an ideal medium. The fluid flow is assumed to be laminar. A coupling model of thermal and flow fields is established based on the Navier-Stokes equations. The system of equations includes the continuity equation, momentum equation, and generalized heat transfer equation, as shown in equation (1) [1].

$$\begin{cases} \nabla \cdot \boldsymbol{u} = 0 \\ \rho \dfrac{\partial \boldsymbol{u}}{\partial t} + \rho(\boldsymbol{u} \cdot \nabla)\boldsymbol{u} = \nabla\left[-p\boldsymbol{I} + \mu(\nabla \boldsymbol{u} + (\nabla \boldsymbol{u})^{\mathrm{T}}\right] + \boldsymbol{F}_{st} + \boldsymbol{F}_e + \boldsymbol{F}_g \\ \rho c \dfrac{\partial T}{\partial t} + \nabla \cdot (-k \nabla T) = Q + h(T_e - T) - \rho c \boldsymbol{u} \cdot \nabla T \end{cases} \tag{1}$$

Where r is the density of the fluid, $\boldsymbol{u}$ is the velocity of the fluid flow, p is the pressure acting on the fluid, $\boldsymbol{I}$ is the unit matrix, m is the dynamic viscosity coefficient of the fluid, $\boldsymbol{F}_{st}$, $\boldsymbol{F}_e$, and $\boldsymbol{F}_g$ correspond to the volume forces, electric field force, and gravity force, respectively, c is the specific heat capacity of the fluid under constant pressure, k is the thermal conductivity, Q is the heat generation efficiency per unit volume of fluid, T is the intrinsic temperature and T_e is the ambient temperature.

2.1.2 Coupled equations for the electric and flow fields

When the transformer is energized, an electric field is generated within its interior. The presence of bubbles in the electric field causes polarization, resulting in the generation of polarization charges on the

ISSN 2706-655X Vol.5, Issue 8: 71-80, DOI: 10.25236/IJFET.2023.050810

surfaces of the bubbles. These charges are subjected to electric field forces, which subsequently influence the shape and motion of the bubbles. Moreover, as the transformer oil flows, it transports the bubbles, thereby subjecting them to the influence of the flow field. Fig. 2 illustrates the coupled model of the electric and flow fields

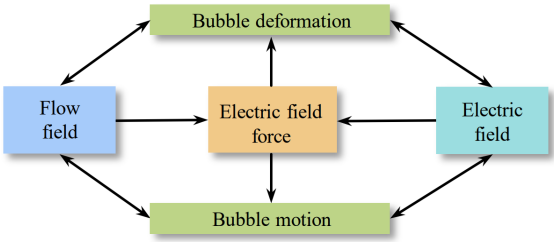

Figure 2: Coupled model of electric and flow fields in transformer oil with bubbles

This paper establishes a coupling relationship between the electric field and the flow field by considering the electric field force. The distribution of polarization charges at the interface between the bubbles and the transformer oil is considered in the analysis. The electric field force, $\boldsymbol{F}_e$, exerted on the fluid can be determined by employing the Maxwell stress tensor, as represented in Equation (2) [10].

$$\boldsymbol{F}_e = \nabla \cdot T \tag{2}$$

Where $\boldsymbol{T}$ is the Maxwell stress tensor. In electrostatic fields, $\boldsymbol{T}$ is determined by the displacement vector $\boldsymbol{D}$ and the electric field strength $\boldsymbol{E}$, and it can be expressed as Equation (3).

$$\boldsymbol{T} = \boldsymbol{E}\boldsymbol{D}^{\mathrm{T}} - \frac{1}{2}(\boldsymbol{E} \cdot \boldsymbol{D})\boldsymbol{I} \tag{3}$$

By substituting Equation (3) into Equation (2), the electric field force $\boldsymbol{F}_e$ can also be expressed as Equation (4).

$$\boldsymbol{F}_e = \nabla \cdot (\boldsymbol{E}\boldsymbol{D}^{\mathrm{T}} - \frac{1}{2}(\boldsymbol{E} \cdot \boldsymbol{D})\boldsymbol{I}) \tag{4}$$

2.1.3 Electric-thermal-fluid multi-physics field coupling model

In the two-phase gas-liquid flow system of transformer oil with bubbles, a complex coupling relationship exists among the electric field, thermal field, and flow field. Firstly, variations in the thermal field affect the dynamic viscosity of the transformer oil, thereby influencing the flow velocity of the oil. The flow velocity of the oil reflects its heat transfer capacity, thereby influencing the temperature distribution within the oil. Consequently, a mutual interaction exists between the thermal field and flow field, forming a coupling relationship. Secondly, variations in the thermal field influence the electrical conductivity and dielectric constant of both the transformer oil and bubbles, consequently impacting the distribution of the electric field. Partial discharge can occur in the bubbles when the electric field intensity reaches a certain level, generating heat that subsequently affects the temperature distribution of the oil. Therefore, there is a mutual interaction between the electric field and the thermal field, forming a coupling relationship. Finally, the deformation and motion of the bubbles are simultaneously affected by the electric field force and fluid drag force. The coupling relationship between the electric field and the flow field is established through the dynamic model of the bubbles. Fig. 3 illustrates the electric-thermal-flow multi-physics field coupling model of transformer oil with bubbles.

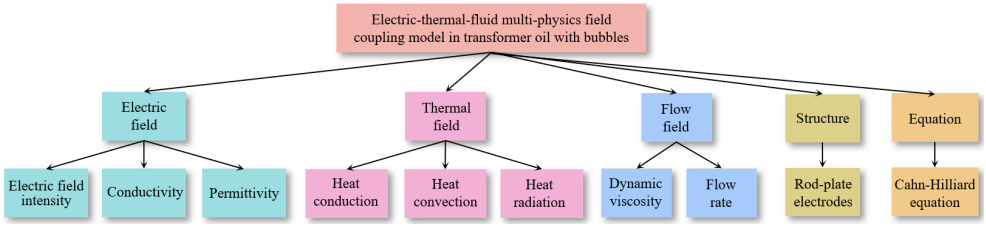

Figure 3: Electric-thermal-fluid multi-physics field coupling model

ISSN 2706-655X Vol.5, Issue 8: 71-80, DOI: 10.25236/IJFET.2023.050810

2.2 Bubble Forces and Development of a Dynamic Model

Bubbles in an oil-immersed transformer experience the dominant forces of electric field force $\boldsymbol{F}_e$, viscous drag force $\boldsymbol{F}_D$, buoyancy force $\boldsymbol{F}_B$, and gravity force $\boldsymbol{F}_g$. Fig. 4 presents a schematic diagram depicting the analysis of forces acting on bubbles at different stages.

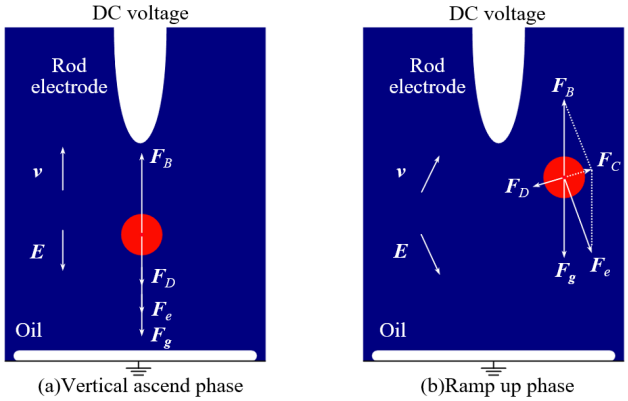

Figure 4: Schematic diagram of force analysis on bubbles under a non-uniform electric field

The dynamic equations governing the motion of bubbles in stationary transformer oil, as well as the mathematical equations describing the electric field force $\boldsymbol{F}_e$, viscous drag force $\boldsymbol{F}_D$, buoyancy force $\boldsymbol{F}_B$, and gravity force $\boldsymbol{F}_g$ acting on the bubbles, are represented by Equation (3) [7].

$$\begin{cases} M_e \dfrac{d\boldsymbol{v}}{dt} = \boldsymbol{F}_e + \boldsymbol{F}_D + \boldsymbol{F}_B + \boldsymbol{F}_g \\ \boldsymbol{F}_e = \nabla \cdot (\boldsymbol{E}\boldsymbol{D}^{\mathrm{T}} - \dfrac{1}{2}(\boldsymbol{E} \cdot \boldsymbol{D})\boldsymbol{I}) \\ \boldsymbol{F}_D = -4\pi\mu r\boldsymbol{v} \\ \boldsymbol{F}_B = \dfrac{4}{3}\pi r^3 \rho_o \boldsymbol{g} \\ \boldsymbol{F}_g = -\dfrac{4}{3}\pi r^3 \rho_g \boldsymbol{g} \end{cases} \tag{5}$$

Where M_e is the effective mass of the bubble during motion, $\boldsymbol{v}$ is the bubble motion velocity, r is the bubble radius, r_o is the density of insulating oil and r_g is the density of air.

2.3 Phase-field Method

Analyzing the motion and deformation characteristics of bubbles is crucial for investigating the impact mechanism of bubbles on the insulating performance of transformer oil. Accurately tracking the variations of the gas-liquid interface is a key aspect. This paper utilizes the phase-field method to precisely track the changes in the gas-liquid interface.

The phase-field method assumes the presence of a transition region with a certain width for incompressible multiphase interfaces. This region experiences interface stresses and diffusion effects between the fluids, which are represented by a continuous phase-field variable denoted as f, $f \in (-1,1)$. The variable remains constant in the two-phase fluids. The coupling solution of the governing equations for the flow field and the interface yields the velocity of the flow field. The fourth-order Cahn-Hilliard equation is then solved to update the phase-field variable in the flow field, enabling the tracking of interface changes [11]. In the paper, the bubble phase is represented by the variable f = -1, while the insulating oil phase is represented by f = 1.

This study employs the Cahn-Hilliard equation to capture the diffusion behavior of the interface by considering the combined effect of interfacial potential and thermodynamic driving forces, as depicted in Equation (6) [12].

ISSN 2706-655X Vol.5, Issue 8: 71-80, DOI: 10.25236/IJFET.2023.050810

$$\begin{cases} \dfrac{\partial \phi}{\partial t} + \boldsymbol{u} \cdot \nabla \phi = \nabla \cdot \gamma \ \nabla G \\ G = \dfrac{3\sqrt{2}\sigma\delta}{4}\left[\dfrac{\phi(\phi^2 - 1)}{\delta^2} - \nabla^2 \phi \right] \end{cases} \tag{6}$$

Where g is the mobility, G is the chemical potential and d is the interfacial thickness.

The expressions for the volume fractions V_o and V_g of transformer oil and gas bubble respectively, the density r , dynamic viscosity m , permittivity e , and conductivity s at the interface, can be obtained as shown in equation (7).

$$\begin{cases} V_o = \dfrac{1+\phi}{2} \\ V_g = \dfrac{1-\phi}{2} \\ \rho = \rho_o V_o + \rho_g V_g \\ \mu = \mu_o V_o + \mu_g V_g \\ \varepsilon = \varepsilon_o V_o + \varepsilon_g V_g \\ \sigma = \sigma_o V_o + \sigma_g V_g \end{cases} \tag{7}$$

3. Construction of the Simulation Model and Analysis of the Results

This study has developed rod-plate electrodes oil channel model based on a two-phase gas-liquid flow, considering the actual structure inside the transformer oil. The model can accurately describe the spatial distribution of non-uniform electric fields. This study aims to investigate the effects of bubble size, number, and different voltage levels on bubble deformation, motion trajectory, and the extent of internal electric field distortion. Table 1 presents the parameters of the transformer oil and air bubbles.

Table 1: Material parameters

Parameters	Numerical value
Transformer oil density (kg/m^{-3})	875
Relative dielectric constant of oil	2.4
Dynamic viscosity of oil (Pa·s)	0.0167
Thermal conductivity of transformer oil (W/(m·k))	0.1065
Gas density in bubbles (kg/m^{-3})	1.205
Relative dielectric constant of bubbles	1
Dynamic viscosity of bubbles (Pa·s)	1.83e-5
Thermal conductivity of bubbles (W/(m·k))	0.295
Surface tension coefficient	0.031

3.1 Effect of Voltage Levels on the Characteristics of Bubble Motion

Based on the aforementioned simulation model and method, the study investigated the motion characteristics of a single bubble with a diameter of 4mm under different direct voltage levels 0kV, 15kV, 30kV, and 45kV as well as its impact on the distortion degree of the internal electric field within the bubble. The simulation results are shown in Fig. 5.

ISSN 2706-655X Vol.5, Issue 8: 71-80, DOI: 10.25236/IJFET.2023.050810

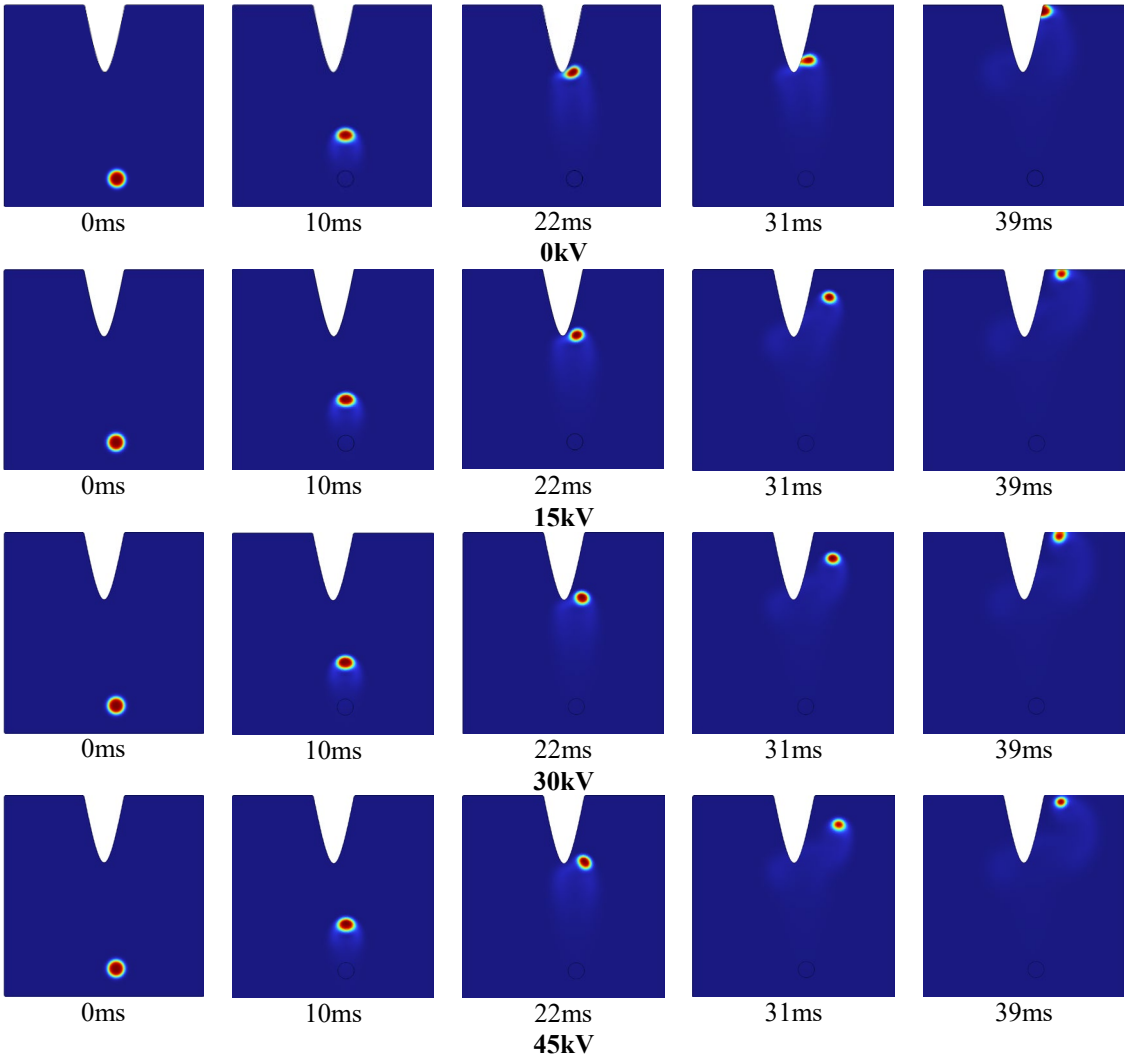

Figure 5: Effect of voltage levels on the trajectory of bubble motion

From Fig. 5, it is evident that during the ascending stage, when the bubble is positioned below the rod electrode, it elongates vertically due to the stretching effect of the electric field force, forming an elliptical shape with the elongation direction perpendicular to the electric field lines. During the sloping stage, as the bubble enters the strong electric field region, it undergoes stretching and experiences repulsion from the strong electric field force, gradually moving away from the rod electrode. With increasing voltage levels, the displacement of the bubble near the rod electrode intensifies, and both the stretching and repulsion directions align parallel to the electric field lines. As the bubble is pushed away from the strong electric field region, its shape gradually transitions from elliptical to circular.

By combining the curve in Fig. 6, it can be inferred that within the time interval of 0ms to 30ms, the bubble ascends and moves closer to the rod electrode, while the maximum electric field intensity inside the bubble gradually increases, albeit at a slow rate. Around 30ms, the bubble reaches its peak in terms of the maximum internal electric field intensity. At this juncture, the bubble experiences the strongest influence from the polarization effect of the electric field near the rod electrode, and the maximum internal electric field intensity increases with higher voltage levels. As the bubble moves away from the strong electric field region, the maximum internal electric field intensity gradually decreases. Additionally, the greater repulsive effect of the electric field force at higher voltage levels quickly pushes the bubble out of the strong electric field region, leading to a faster decrease in the maximum internal electric field intensity.

ISSN 2706-655X Vol.5, Issue 8: 71-80, DOI: 10.25236/IJFET.2023.050810

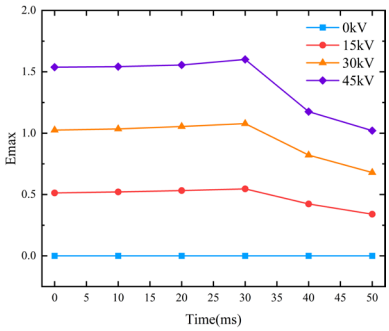

Figure 6: Variation curve of the maximum electric field intensity within bubbles at different voltage levels

3.2 Effect of Bubble Size on the Characteristics of Bubble Motion.

Based on the aforementioned simulation model and method, the motion characteristics of single bubbles with diameters of 4mm, 4.5mm, and 5mm are studied under a 15kV direct voltage, along with their impact on the degree of internal electric field distortion within the bubbles. The simulation results are shown in Fig. 7.

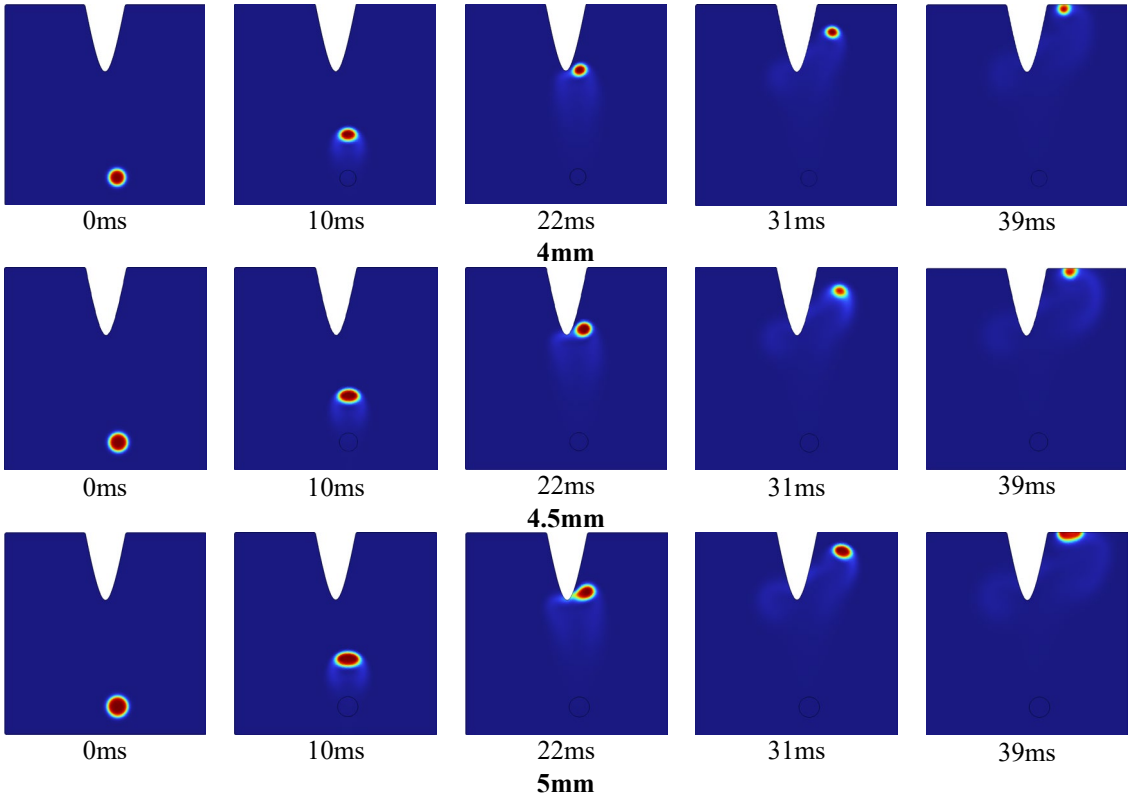

Figure 7: Effect of bubble size on the trajectory of bubble motion

From Fig. 7, it is observed that during the ascending phase, when the bubble is positioned below the rod electrode, it undergoes stretching deformation vertically due to the vertical electric field force. The bubble takes on an elliptical shape, and the degree of vertical compression deformation increases with larger bubble sizes. During the ramp-up phase, as the bubble enters the strong electric field region, it experiences stretching and repulsion forces from the strong electric field, causing it to gradually move away from the rod electrode. Additionally, larger bubbles demonstrate higher overall speeds during the ramp-up phase. Subsequently, as the bubble is pushed away from the strong electric field region, its shape gradually transitions from elliptical to circular. Larger bubbles require a longer transition time from elliptical to circular shapes.

By analyzing the curve in Fig. 8, it is concluded that during the 0ms to 30ms timeframe, the bubble ascends and approaches the rod electrode, resulting in a gradual increase in the maximum internal electric

ISSN 2706-655X Vol.5, Issue 8: 71-80, DOI: 10.25236/IJFET.2023.050810

field intensity, albeit at a slow rate. At approximately 30ms, the bubble reaches its peak value for the maximum internal electric field intensity, indicating its highest influence from electric field polarization near the rod electrode. Moreover, larger bubbles demonstrate higher peak values of the maximum internal electric field intensity. Subsequently, as the bubble moves away from the strong electric field region, the maximum internal electric field intensity gradually decreases. From 35ms to 40ms, the rate of decrease is significantly influenced by the bubble's deformation recovery time. Larger bubbles encounter stronger inertial effects, resulting in a longer transition time from elliptical to circular shape and, consequently, a slower decrease in the maximum internal electric field intensity. However, from 40ms to 50ms, the rate of decrease is primarily determined by the overall speed of the ramp-up phase. Larger bubbles, due to their higher overall speeds during the ramp-up phase, experience a faster decrease in the maximum internal electric field intensity as they are pushed away from the strong electric field region.

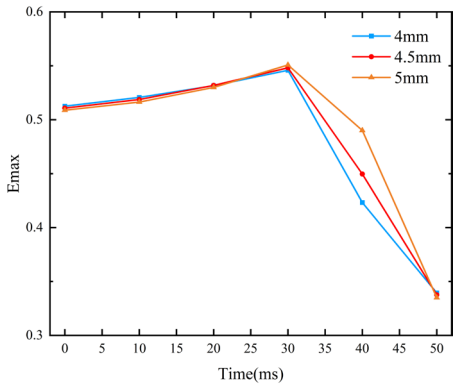

Figure 8: Variation curve of maximum electric field intensity within bubbles of different sizes

3.3 Effect of the Bubble Number on the Characteristics of Bubble Motion

Based on the aforementioned simulation model and method, the motion characteristics of single bubble, double bubbles, and triple bubbles with a diameter of 4mm were separately investigated under a 15kV direct voltage, along with their impact on the internal electric field distortion of the bubbles. The simulation results are shown in Fig. 9.

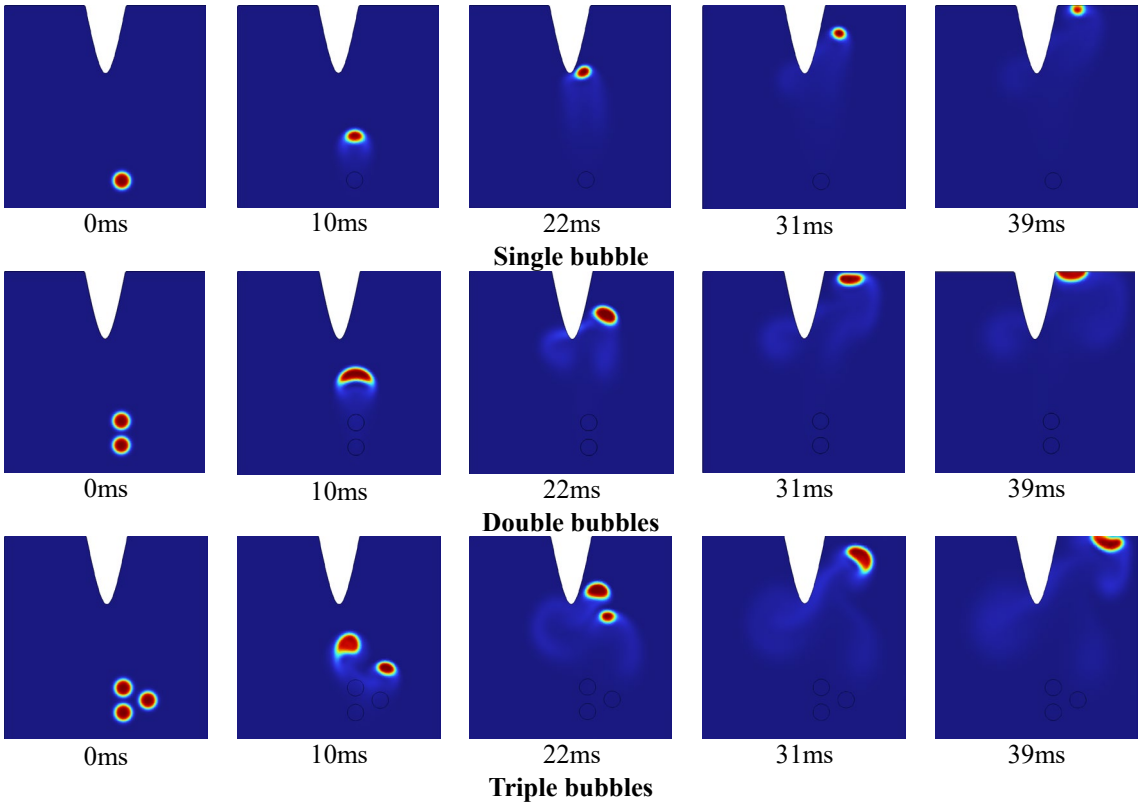

Figure 9: Effect of bubble number on the trajectory of bubble motion

ISSN 2706-655X Vol.5, Issue 8: 71-80, DOI: 10.25236/IJFET.2023.050810

The motion of a single bubble corresponds to the previous analysis, and it will not be reiterated here. From Fig. 9, it can be observed that in the case of two bubbles, they undergo coalescence at 10ms and are subjected to elongation by the vertical electric field, forming a cap-like shape. In the case of three bubbles, at 10ms, the two bubbles in the same vertical direction first undergo coalescence, and at 31ms, the combined structure of the two bubbles merges with the third bubble. Moreover, as the number of bubbles increases, the size of the merged bubble enlarges, resulting in a significant increase in terms of the overall speed during the ramp-up phase and an extended transition time from an elliptical to a circular shape.

Based on the curves in Fig. 10, it can be concluded that the maximum internal electric field strength is 0.545 kV/mm for a single bubble, 0.536 kV/mm for two bubbles, and 0.554 kV/mm for three bubbles. The fluctuation in the peak value of the maximum internal electric field strength is attributed to the irregular shape variations that occur when multiple bubbles coalesce, leading to an irregular distribution of surface polarized charges. However, the overall trend of the maximum internal electric field strength still increases with an increasing number of bubbles.

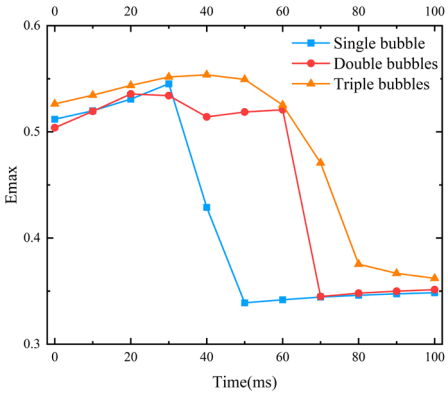

Figure 10: Variation curve of maximum electric field intensity within bubbles of different numbers

4. Conclusion

In this study, a two-phase flow model with rod-plate electrodes was constructed based on the phase-field method to characterize the spatial distribution of non-uniform electric fields under the coupled effects of electric, thermal, and fluid fields. Numerical simulations were performed to analyze the effects of bubble size, number, and different voltage levels on bubble deformation, motion trajectory, and the extent of internal electric field distortion, leading to the following conclusions:

(1) During the vertical ascent phase, the bubbles undergo deformation perpendicular to the electric field direction, and during the ramp-up phase, they deform along the electric field direction. With an increase in voltage level, the stretching and repulsion of the bubbles by the electric field force also increase.

(2) There is a positive correlation between bubble size, voltage level, and the degree of distortion of the maximum electric field strength inside the bubbles. Coalescence of multiple bubbles leads to irregular shape changes and non-uniform distribution of polarized charge on their surface. However, the internal maximum electric field strength tends to increase with an increasing number of bubbles.

References

[1] Zhang Ning, Liu Shili, Hao Jian, et al. Review on Partial Discharge Characteristics of Bubble Impurity Phase in Transformer Oil [J]. Transactions of China Electrotechnical Society, 1-20 [2023-01-20].

[2] Gao M, Zhang Q, Ni H, et al. Study on gas bubble formation in single-layer paper insulation [C]// 2017 1st International Conference on Electrical Materials and Power Equipment (ICEMPE). Xi'an, China: IEEE, 2017: 283-286.

[3] Liao Ruijin, Lin Yuandi, Yang Lijun, et al. Effects and Correction of Temperature, Moisture and Aging on Furfural Content in Insulating Oil and Aging Assessment of Insulation Paper[J]. Proceedings of the CSEE, 2017, 37(10): 3037-3044.

[4] Hill J P, Wang Z, Liu Q, et al. Improvements to the Construction of Bubble Inception Formulae for

ISSN 2706-655X Vol.5, Issue 8: 71-80, DOI: 10.25236/IJFET.2023.050810

Use With Transformer Insulation[J]. IEEE Access, 2019, 7: 171673-171683.
[5] Liu Y, Chao N, Zhao T, et al. Mechanism and numerical model of bubble effect in oil-paper insulation based on microtubule model[J]. IEEE Transactions on Dielectrics and Electrical Insulation, 2020, 27(5): 1529-1537.
[6] Zhao Tao, Liu Yunpeng, Lü Fangcheng, et al. Bubble Dynamics Simulation in Transformer Oil under AC Electric Field[J]. Journal of System Simulation, 2016, 28(12): 3081-3086+3094.
[7] Liu Qiushi, Li Qingmin, Niyomugabo E.Ladislas, et al. Bubble Dynamics and Migration Mechanism in Insulation Oil Under Extremely Inhomogeneous Electric Field[J]. Proceedings of the CSEE, 2021, 42(9): 3460-3470.
[8] Yang Hao, Zhao Heng, Zhang Lu, et al. Motion Characteristics of Bubbles in Oil Paper Insulation Structure Under Extremely Inhomogeneous Electric Field[J]. Southern Power System Technology, 2022, 16(5): 79-86.
[9] Ladislas N E, Li Q, Liu Q, et al. Bubble migration characteristics in power transformer oil under coupled stresses of forced vibration and electrical field[J]. IET Science, Measurement & Technology, 2022: smt2.12136.
[10] Zhang Yongze, Tang Ju, Pan Cheng, et al. Simulation of the Bubble Dynamics and Electric Field Distribution in Flowing Transformer Oil [J]. High Voltage Engineering, 2020, 46(6): 2004-2012.
[11] Han Dan, Study on the Calculation Method of Two-phase Flow under Electric Field, A thesis submitted in partial satisfaction of the Requirements for the degree of Master of Engineering in Communication and Information System in the School of Computer and Communication Lanzhou University of Technology, April. 2019.
[12] Zhang Yongze, Investigation of the PD and Breakdown Characteristics in Flowing Transformer Oil Containing Bubbles, A Dissertation Submitted to Chongqing University In Partial Fulfillment of the Requirement for the Doctor's Degree of Engineering, December. 2019.